ELSEVIER

Intermetallics 10 (2002) 1105–1112

Intermetallics

www.elsevier.com/locate/intermet

Oxygen impurity and microalloying effect in a Zr-based bulk metallic glass alloy

C.T. Liu*, M.F. Chisholm, M.K. Miller

Oak Ridge National Laboratory, Oak Ridge, TN 37830-6115, USA

Received in revised form 2 July 2002; accepted 2 July 2002

Abstract

A Zr-base bulk metallic glass (BMG) alloy with the base composition Zr–10 at.%Al–5% Ti–17.9% Cu–14.6% Ni (BAM-11) was used to study the effects of oxygen impurities and microalloying on the microstructure and mechanical properties. Oxygen impurity at a level of 3000 appm dramatically reduced the glass forming ability and embrittled BAM-11 at room temperature. The embrittlement was due to the formation of oxygen-induced Zr_4Ni_2O nuclei that triggered near complete crystallization of the metallic glass. Microalloying with 0.1 at.%B + 0.2%Si + 0.1%Pb was effective in suppressing the crystalline phase formation and alleviating the detrimental effect of oxygen. Microstructural analyses indicate that the beneficial effect of the optimum dopants was mainly due to stabilization of the glass-phase matrix even though it contained high levels of oxygen. Thus, microalloying is effective in reducing the production cost and is very useful for manufacturing good-quality Zr-based BMGs from impure charge materials.
© 2002 Published by Elsevier Science Ltd.

Keywords: B. Glasses, metallic; Mechanical properties at ambient temperatures; D. Phase interface; F. Atom microprobe; Electron microscopy, scanning

1. Introduction

Bulk Metallic Glasses (BMGs) constitute a new and exciting class of materials with unique physical and mechanical properties for structural and functional use [1,2]. Among all BMGs, multicomponent alloys based on Zr have superior glass forming ability (GFA), and they can be readily produced into parts with cross sections larger than a few centimeters by conventional melting and casting techniques. In multicomponent systems, GFA can be simply viewed as the resistance to the precipitation of crystalline phases from undercooled liquids [3,4]. Both major alloying elements and minor alloying additions affect the crystallization process in BMGs. Inoue has suggested three empirical rules apply to alloys that have high GFA: [1] at least three alloying elements, [2] large mismatch in atomic sizes of constituent elements, and [3] large negative heat of mixing among major alloying elements [1,5].

In comparison with major elements, minor alloying additions (or impurities) have been also found to be equally important for the GFA and thermal stability of BMGs. Lin, Johnson, and Rim [6] discovered that oxygen additions strongly affect the critical cooling rate for glass formation in a Zr-based alloy. The nose of the crystalline phase stability region on temperature–transformation–time (TTT) curves shifts to higher temperatures and shorter times with increasing oxygen content. Eckert et al. [3] and Gebert et al. [4] reported that oxygen impurities in Zr-based BMGs changed the crystallization processes from a single to a double stage, thereby reducing the supercooled liquid region [defined as the difference between the crystallization temperature (T_x) and the glass transition temperature (T_g)]. Atom probe studies [7–9] indicated that oxygen redistribution took place during the crystallization reaction and thus influenced the kinetics of crystallization in Zr–Cu–Al–Pd BMGs. Oxygen-induced precipitation of metastable quasicrystalline phases has been observed in a number of Zr-based BMGs reported recently [3,4,10–12]. All of these indicate the adverse effects of oxygen on the GFA and thermal stability of BMGs.

Zr-based BMGs lose their excellent GFA when the oxygen impurity level is high (> 1000 appm); as a result, high-purity, high-cost materials (such as pure Zr) have to be used for manufacturing. Recent studies indicate

* Corresponding author. Tel.: +1-865-574-4449; fax: +1-865-574-7659.

E-mail address: liuct@ornl.gov (C.T. Liu).

0966-9795/02/$ - see front matter © 2002 Published by Elsevier Science Ltd.
PII: S0966-9795(02)00131-0

that the harmful effect of oxygen can be reduced to a certain extent by macroalloying (>1 at.%). Zhang et al. [13] reported that the GFA of Zr–Al–Ni–Cu alloys with oxygen impurities could be improved by alloying with 2–4% Y. Also, Liu et al. [14] indicate that a 2% increase of Al content greatly reduces the crystalline phase formation in a well developed Zr-based BMG alloy containing high levels of oxygen. Micro alloying with <1% alloy additions has been proved to be effective in taking care of some material problems in crystalline alloys [15,16]. The objective of this research is to explore and to understand the role of microalloying additions in reducing or eliminating the harmful effect of ⩾0.2 at.% O in a Zr-based alloy. This work demonstrates that microalloying can be very effective in suppressing the crystalline phase formation and alleviating the detrimental effect of oxygen impurity.

2. Experimental procedures

A Zr-based alloy with the composition Zr–10 at.% Al–5% Ti–17.9% Cu–14.6% Ni (heat number: BAM-11) was used as the base alloy in the current study. This alloy was developed at Caltech, with a trade name of Vitreloy 105. Three microalloying elements, B, Si and Pb, were chosen to add to the base composition for the study of microalloying effects. The idea is that these elements have a strong tendency to form oxygen-rich glass phases (e.g. borosilicates). These oxide glasses also have relatively low melting points that are comparable to that of the metallic glass. The various combinations of dopants added to the base composition are listed in Table 1. All alloys were prepared by arc melting and drop casting into a copper mold with 6.4 mm diameter and 76.2 mm length. Both commercial purity Zr metal containing 4460 appm O and high purity Zr metal with 560 appm O were used for alloy preparation. Wet chemical analyses indicated that pure alloy (PA) ingots contained ~590 appm O and the commercial purity alloys (CA) ingots contained ~3000 appm O.

Table 1
Microalloying elements added to the base alloy, BAM-11 (Zr–10% Al–5% Ti–17.9% Cu–14.6% Ni)

Alloy No.	Dopant concentrations (%)
BAM-11	Base composition
BAM-31	0.05% B
BAM-23	0.10% B
BAM-24	0.20% B
BAM-25	0.30% B
BAM-40	0.10% Si
BAM-38	0.10% B + 0.05% Si
BAM-37	0.10% B + 0.10% Si
BAM-39	0.10% B + 0.20% Si
BAM-44	0.10% Pb
BAM-42	0.10% B + 0.20% Si + 0.05% Pb
BAM-41	0.10% B + 0.20% Si + 0.10% Pb
BAM-43	0.10% B + 0.20% Si + 0.20% Pb

Microstructural features and tensile properties were all determined from as-cast ingots. X-ray diffraction confirms the formation of amorphous structures in PA materials [17]. Metallographic samples were polished on Syntron machines and etched in a solution of 40-ml HNO_3 plus 10 drops of HF. The microstructure and composition were analyzed by wavelength dispersive spectroscopy and energy dispersive spectroscopy using an electron microprobe operating at ⩽20 kV. Tensile specimens with a 3.19 mm gauge diameter were fabricated by centerless grinding. Tensile tests were conducted at room temperature with a strain rate of 3.3×10^{-3} s^{-1}; the fracture strength was calculated from the load–time curves. Field ion micrographs were recorded with the use of neon as the image gas and with a specimen temperature of 60 K. Atom probe analysis was performed in an energy-compensated optical position-sensitive atom probe under ultra high vacuum with a specimen temperature of 60 K, a pulse repetition rate of 1.5 kHz and a pulse fraction of 20%. Specimens for electron microscopy were prepared by electro-polishing (1 part sulfuric acid and 7 parts methanol at 25 °C) and then ion milled using low energy (500 eV) Ar^+ ions while cooling the specimen with liquid nitrogen. The specimens were examined using a Vacuum Generators HB-603U scanning transmission electron microscope (STEM) operated at 300 kV.

3. Results

3.1. Microstructural analyses

The microstructure of the alloy ingots was examined by both optical metallography and electron microscopy. The microstructures near the ingot central region of PA BAM-11 with 590 ppm O and CA material with 3000 ppm O are compared in Fig. 1. No microstructural features (such as grain boundaries) were detected in the PA material (Fig. 1a), indicating the formation of the glass phase. In contrast, nearly complete crystallization with grain size around 10 μm is observed in the CM material with the high oxygen content. The amount of the crystalline phases decreases with the distance away from the ingot center. This decrease is apparently due to cooling rate effects. A mixture of two major phases, i.e., crystalline-phase particles dispersed in the glass phase matrix, is observed in the near surface region of the ingot, as shown in Fig. 2. Crystallographic features are also seen in some crystalline particles. It is important to point out that small particles with a bright contrast were detected near the center of some of the crystallized regions (see upper left in Fig. 2). Electron microprobe analyses show that these small, bright appearing parti-

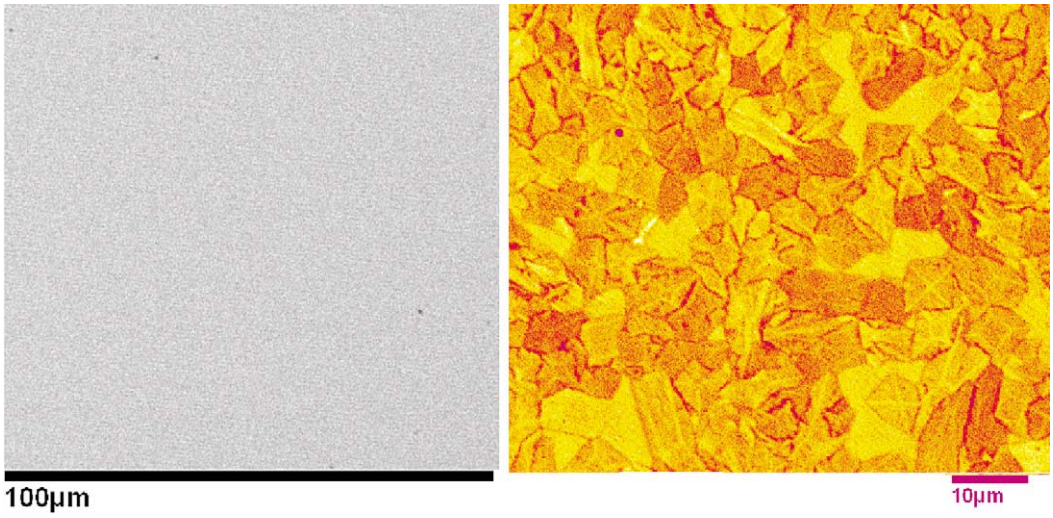

Fig. 1. Back-scattered electron micrographs of (a) PA BAM-11 (590 appm O) and (b) CA BAM-1 (3000 appm O) near ingot central region.

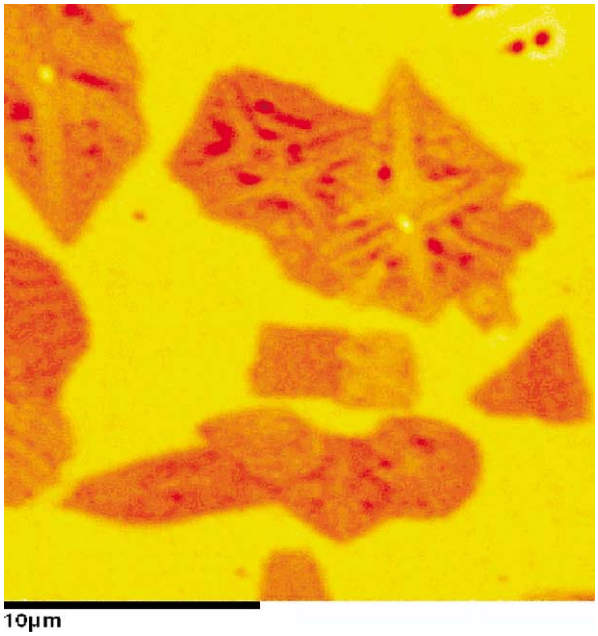

Fig. 2. Back-scattered electron micrograph of CA BAM-11 (3000 appm O) near the ingot surface.

cles are enriched with Ni and depleted in Cu and Ti, as indicated in the compositions (in atomic %) given below: small bright particles: Zr–11.3% Al–17.2% Ni–3.0% Ti–15.8% Cu crystallized region: Zr–11.5% Al–15.4% Ni–4.6% Ti–18.2% Cu.

Note that, because of their small size, the exact composition of these particles can not be determined by electron microprobe analysis. The amorphous phase is essentially formed in all PA materials with various dopants listed in Table 1. The effects of dopants on the microstructure of the CA materials with different dopants can be seen in Fig. 3. The addition of 0.1 at.%B and 0.2% Si significantly reduces the amount of crystalline phases in the ingot central region and some retained glass phase regions are observed (Fig. 3b). Note that the size of the crystalline particles does not appear to be affected by the dopants. Most significantly, microalloying with 0.1% Pb dramatically reduces both the amount and the size of crystallized regions (Fig. 3c). As indicated in Fig. 3d, crystallization of the glass is essentially suppressed by microalloying with the combination: 0.1% B + 0.2% Si + 0.1% Pb. These observations show clearly the beneficial effect of dopants on suppression of the formation of crystalline phases in BAM-11 containing a high level of oxygen.

3.2. Tensile results

The room-temperature tensile strengths of PA BAM-11 and CA BAM-11 with and without dopants are summarized in Table 2. The PA material showed an elastic deformation of approximately 2% (17), followed by catastrophic failure with a high fracture strength of 1760 MPa. In contrast, the CA material without the dopants was so brittle that it actually fractured during specimen preparation (i.e., fracture strength 0 MPa). The addition of B and Si dopants alone and in combination resulted in no improvement in fracture strength. Only Pb was found to be effective in restoring the fracture strength of the alloy. It appears that when combined with B and Si, 0.05 at.% Pb is not enough and 0.2 at.% is too much. A maximum fracture strength of 1520 MPa was obtained in the CA material doped with 0.1% B + 0.2% Si + 0.1% Pb (BAM-41). Hence, Pb is most effective in improving the tensile fracture strength of CA BAM-11.

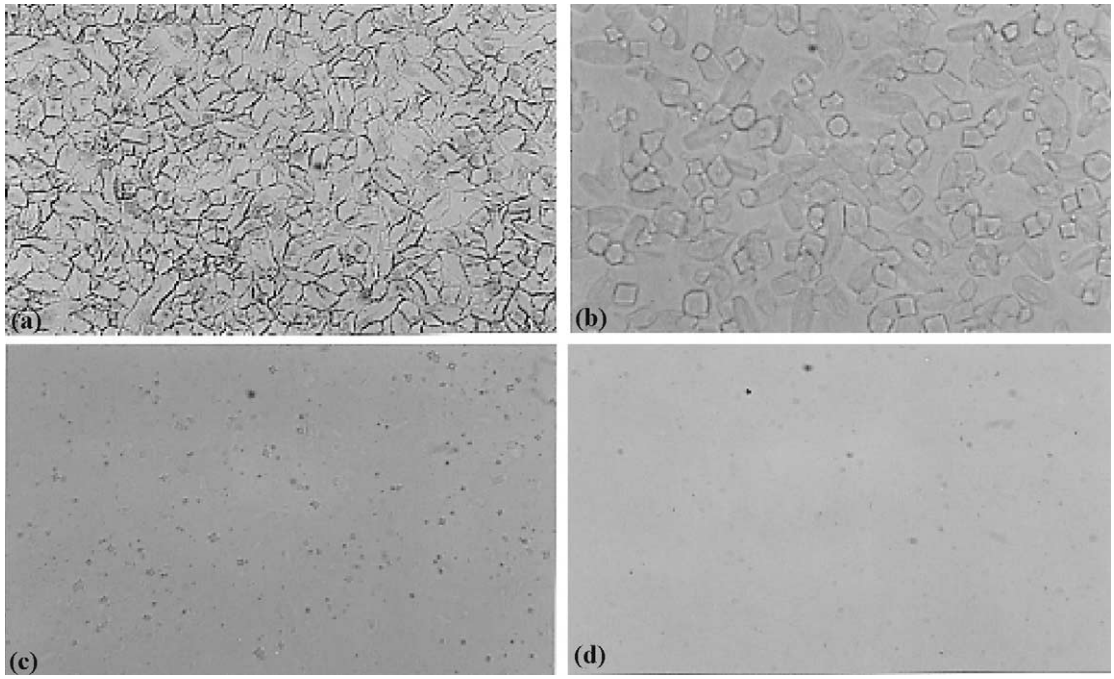

Fig. 3. Micrographs of CA materials: (a) BAM-11, (b) BAM-39, (c) BAM-44, and (4) BAM-41.

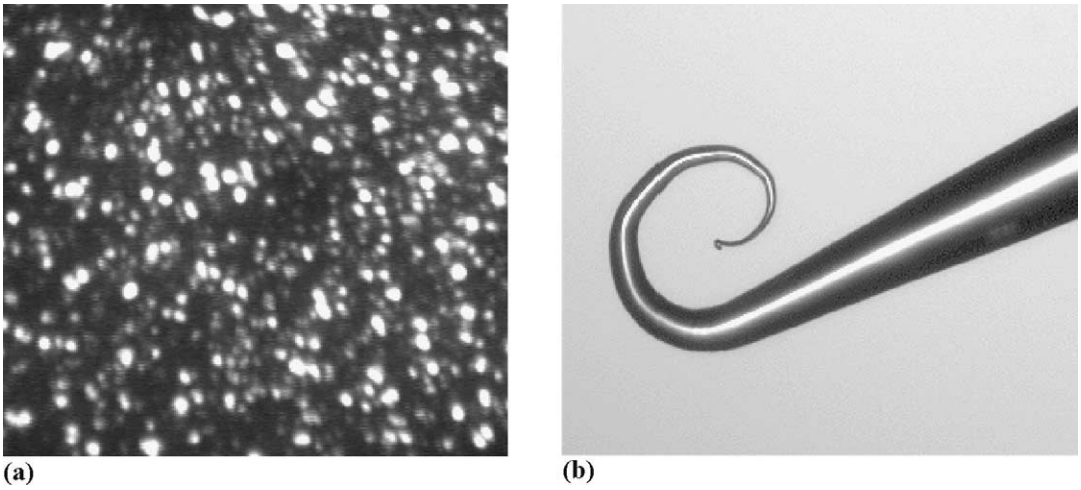

Fig. 4. (a) Field ion micrograph showing the random distribution of atoms in CA BAM-41 and (b) optical micrograph of a bent needle-shaped field ion microscope sample after an accident.

Table 2
Room-temperature tensile properties of BAM-11 microalloyed with various dopants

Alloy number	Purity[a]	Dopant concentration (%)	Fracture strength (MPa)
BAM-11	PA	None (base composition)	1760
BAM-11	CA	None	~0
BAM-23	CA	0.1% B	~0
BAM-40	CA	0.1% Si	~0
BAM-37	CA	0.1% B–0.15% Si	~0
BAM-39	CA	0.1% B–0.20% Si	~0
BAM-42	CA	0.1% B–0.20% Si–0.05% Pb	285
BAM-41	CA	0.1% B–0.20% Si–0.10% Pb	1520
BAM-43	CA	0.1% B–0.20% Si–0.20% Pb	1300

[a] PA = 590 ppm O; CA = 3000 ppm O.

3.3. Atom probe analyses

In order to understand the beneficial effect of the optimum dopants (0.1% B + 0.2% Si + 0.1% Pb), a total of ~25 needle specimens of CA BAM-41 were analyzed using the atom probe facility at ORNL. All field ion micrographs showed a random distribution of atoms, indicating an amorphous structure (Fig. 4a). No grain boundaries, dislocations and other crystalline features were detected in the amorphous matrix. It is interesting to point out that CA BAM-41 is highly ductile, as evidenced in Fig. 4b showing a needle-shaped field ion specimen accidentally heavily bent.

Table 3
Atom probe analyses of the composition (in atomic percent) of the glass matrix of CA BAM-41

Element	Nominal	Matrix
Zr	Balance	Balance
Al	9.9	8.9±0.2
Ti	5.0	5.0±0.2
Ni	14.6	15.1±0.2
Cu	17.8	16.6±0.2
B	0.1	0.05±0.02
Si	0.2	0.21±0.04
Pb	0.1	0.10±0.04
O	0.3	0.47±0.04

The composition of the amorphous matrix phase was carefully analyzed by atom probe, and the result is summarized in Table 3. Statistical analysis of the data found no evidence of fine-scale phase separation in the amorphous matrix, indicating that the amorphous phase is uniform in composition. A comparison of the nominal and analyzed compositions in Table 3 reveals small depletions of the Al and Cu concentrations and a slight increase of Ni concentration in CA BAM-41 ingot. Note that the oxygen content could not be accurately determined in this case because of the overlap of oxygen and titanium intensities.

3.4. Scanning transmission electron microscopic analysis

The commercial purity materials were further characterized by scanning transmission electron microscopy. Both oxygen containing specimens with and without the microalloying additions were found to contain a small number of cube-shaped particles. Most had diameters in the 20–50 nm range with an occasional 100 nm particle. In the z-contrast mode, these particles always appeared darker than the surrounding matrix, indicating a lower average atomic number than the matrix (Fig. 5). Electron diffraction patterns obtained from <100>, <110>, and <111> zone axes suggest that these particles are face-centered cubic (fcc) with d3m symmetry and have a lattice parameter of 1.22 nm. These match the structure of the Zr_4Ni_2O phase first reported by Mackay et al. [18]. It has been found that this Ti_2Ni-type intermetallic phase forms in Zr-based alloys only in the presence of oxygen [18].

It is important to note that these small particles do not serve as nuclei for the formation of large crystalline phases in CA BAM-41 with the microalloying additions. This is in contrast to the behavior of the bright-contrast dots (or small particles) formed in CA BAM-11 without the dopants (Fig. 2). In order to study interfacial structures in detail, both bright field contrast and Z contrast were employed to examine crystalline particle/amorphous matrix interfaces at high magnifications. As shown in Fig. 6, no obvious segregation of high Z elements (e.g. Pb) that would appear bright or low Z elements (e. g. B) that would appear dark at the interface. The Z-contrast images also indicate that the interfacial boundary is not planar on the atomic scale. (Fig. 6b).

4. Discussion

Lin et al. [6] first reported that oxygen at levels of 5000 appm could increase the critical cooling rate of a Zr-based BMG by several orders of magnitude. Our study of BAM-11 indicates that oxygen at a level of 3000 appm results in complete crystallization in the central region of the 6.4 mm ingot where the cooling

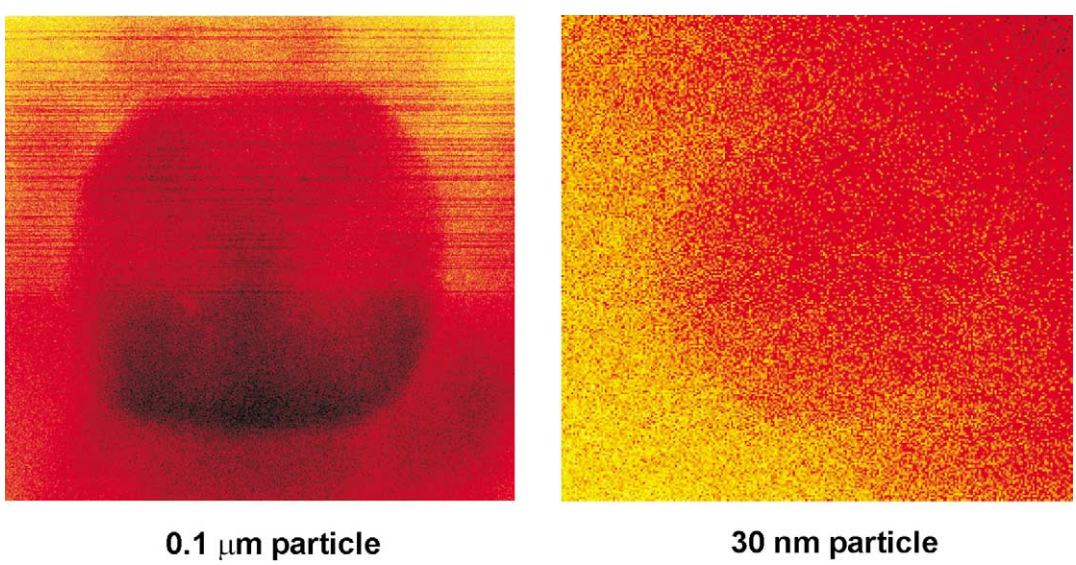

Fig. 5. Z-contrast imaging of tiny crystalline particles showing lower average atomic number than the glass matrix of CA BAM-41.

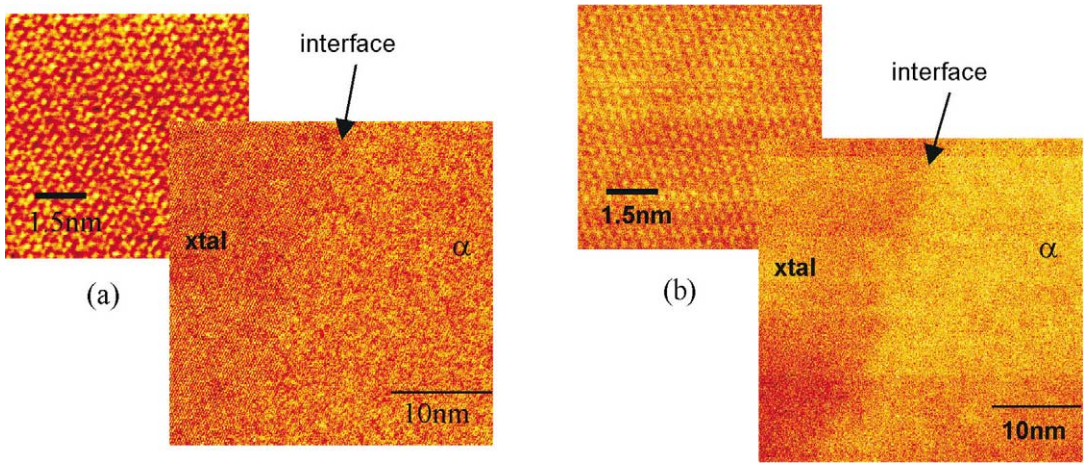

Fig. 6. Scanning transmission electron micrographs showing crystal/amorphous matrix interfaces in CA BAM-41.

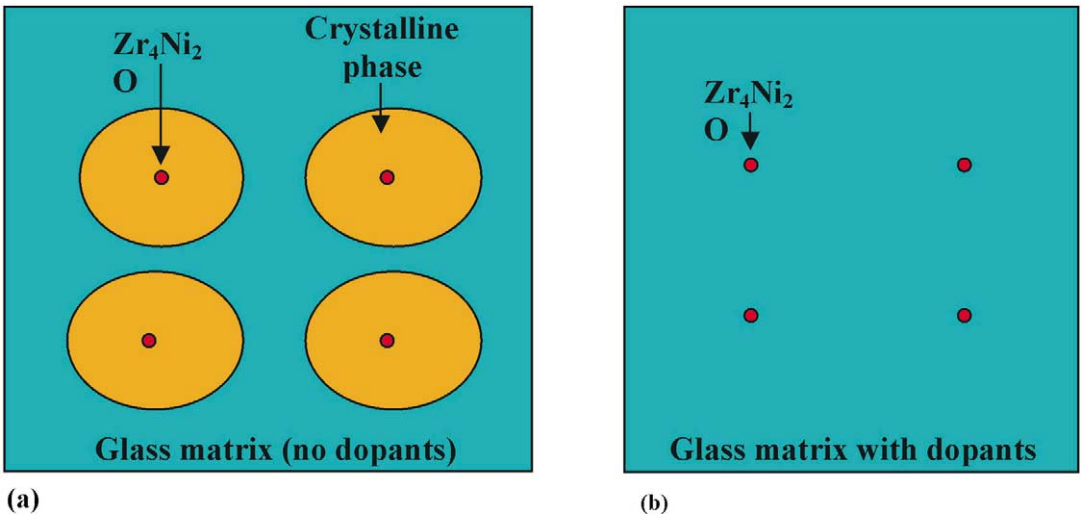

Fig. 7. Sketch to show the beneficial effect of the optimum dopants: (a) CA BAM-11 (no dopants) and (b) CA BAM-41 with 0.1% B + 0.2% Si + 0.1% Pb dopants.

rate is slower than at the surface of the ingot. Comparison of the thickness of the glass phase in the PA and CA ingots suggests that the increase in oxygen from 590 to 3000 appm will increase the critical cooling rate by at least an order of magnitude.

Our study of microstructural features in PA and CA materials suggest that oxygen triggers the nucleation of crystalline nuclei which act as heterogeneous nucleation sites for subsequent formation of large crystalline regions in CA BAM-11 (see Fig. 2). Electron microprobe analyses reveal that these nuclei are enriched in Ni and depleted in Cu. These results are consistent with our electron diffraction analysis and suggestion that the small particles are Zr_4Ni_2O. They are most likely the same "fcc $NiZr_2$-type crystalline phase" formed in Zr–Al–Cu–Ni metallic glasses containing high levels of oxygen, as reported by Eckert et al. [3] and Gebert et al. [4]. The redistribution of oxygen was detected in Zr-based BMGs during crystallization processes [7–9]. Mechanistically, these observations suggest that the detrimental effect of oxygen is due to the formation of oxygen-induced nuclei which serve as nucleation sites for subsequent crystallization of the glass phase.

The atom probe study revealed a random distribution of atoms in the glass matrix of CA BAM-41 microalloyed with the optimum amount of dopants. There was no evidence of any clustering or spinodal decompostion reaction. Instead, small crystalline particles were detected in microalloyed CA BAM-41, which were identified as Zr_4Ni_2O phase by electron diffraction, similar to the results for CA BAM-11. A sketch illustrating the difference in structural features observed in the CA materials without (BAM-11) and with (BAM-41) the optimum dopants is shown in Fig. 7. In both materials, tiny Zr_4Ni_2O particles are formed; however, in the microalloyed material,these particles do not trig-

ger the formation of large crystalline phases around them Two possible factors may contribute to this difference. One is that the segregation of the dopants on Zr_4Ni_2O interfaces may change interfacial structure and chemical composition, thus resulting in suppression of the formation of crystalline phases around them. The z-contrast images (Fig. 6) show no evidence for this segregation. The other is that the dopants strongly stabilize the glass matrix phase containing oxygen to the point where the Zr_4Ni_2O particles no longer trigger crystallization of the metallic glass. Based on these results, we thus conclude that the major beneficial effect of the optimum dopants, 0.1% B + 0.2% Si + 0.1%Si, is to effectively improve the stability of BAM-11 metallic glass containing a high level of oxygen. Further study is certainly required to show how these dopants mechanistically affect the GFA and thermal stability of the glass phase.

Tensile tests indicate that oxygen badly embrittles BAM-11 at room temperature (Table 2). The embrittlement is apparently due to the formation of brittle crystalline phases in CA materials. Note that even small amounts of crystalline particles significantly lower the fracture strength of microalloyed CA materials (such as BAM-42). It is important to point out that microalloying with 0.1B + 0.2Si + 0.1Pb completely suppresses the crystallization reaction in the CA material and restores almost all the fracture strength (as compared with the PA material).

This study shows that Zr-based BAM-11 loses its superior GFA when the oxygen impurity level is high. Because of the harmful effect of oxygen, high-purity Zr metal and high vacuum processing would be required for manufacturing BMG parts with large cross sections. This would substantially increase the material and processing costs. For instance, the market price of commercial-pure Zr metal is on the order of $50 per lb, but it increases to more than $500 per lb for pure Zr required for producing glass material. This study has demonstrated that microalloying is very effective in eliminating the detrimental effect of oxygen and, thus, reducing the manufacturing cost.

5. Conclusions

The study of oxygen impurity and microalloying effect in Zr-based BAM-11 has led to the following conclusions:

1. Oxygen impurity dramatically reduces GFA and embrittles Zr-based BAM-11.
2. Microalloying with 0.1% B + 0.2% Si + 0.1% Pb is very effective in suppressing crystallization of the metallic glass and alleviating the detrimental effect of oxygen.
3. Tiny Zr_4Ni_2O particles with a fd3m symmetry have been identified by electron diffraction. These particles serve as nuclei that trigger the crystallization of CA BAM-11 with high oxygen levels but not in CA BAM-41 microalloyed with the optimum dopants.
4. Atom probe characterization shows no evidence of compositional variation in the glass matrix, indicating no separation of two glass phases in microallyed BAM-41 containing oxygen.
5. These studies suggest that the beneficial effect of the optimum dopants is mainly due to stabilize the glass-phase matrix even containing high oxygen.
6. The tensile properties of the microalloyed CA material are comparable to that of the PA material.
7. This study has demonstrated that microalloying allows the use of commercial purity materials in manufacturing Zr-based BMGs. This will result in reduced materials cost and less stringent casting conditions for Zr-based metallic glass.

Acknowledgements

Research at the Oak Ridge National Laboratory and the SHaRE Collaborative Research Center at ORNL was sponsored by the Division of Materials Sciences and Engineering, U.S. Department of Energy, under contract DE-AC05-00OR22725 with UT-Battelle, LLC.

References

[1] Inoue A. Stabilization of metallic supercooled liquid and bulk amorphous alloys. Acta Mater 2000;48:279–306.
[2] Johnson WL. Bulk amorphous metal—an emerging engineering material. JOM 2002;March:40–3.
[3] Eckert et al J. Crystallization behavior and phase formation in Zr-Al-Cu-Ni metallic glass containing oxygen. Materials Transactions, JIM 1998;39(6):623–32.
[4] Gebert A, Eckert J, Schultz L. Effect of oxygen on phase formation and thermal stability of slowly cooled $Zr_{65}Al_{7.5}Cu_{17.5}Ni_{10}$ metallic glass. Acta Mater 1998;46(15):5475–82.
[5] Inoue A. Mater Sci Engr 1997;A226-228:357.
[6] Lin XH, Johnson WL, Rhim WK. Effect of oxygen impurity on crystallization of an undercooled bulk glass forming Zr-Ti-Cu-Ni-Al alloy. Materials Transactions, JIM 1997;38(5):473–7.
[7] D. H. Ping, K. Hono and A. Inoue, Oxygen distribution in $Zr_{65}Cu_{15}Al_{10}Pd_{10}$ nanocrystalline alloys. Materials Science Forum, 1999;307–31–6.
Journal of Metastable and Nanocrystalline Materials, 1999, 1:31–6. Trans Tech Publications, Switzerland.
[8] Ping DH, Hono K, Inoue A. In: Bulk metallic glasses. MRS vol. 554. Johnson WL, Inoue A, Liu CT, editors. Warrendale (PA): MRS Publication; 1999. p. 3–8.

[9] Chen et al MW. Impurity oxygen redistribution in a nanocrystallized $Zr_{65}Cr_{15}Al_{10}Pd_{10}$ metallic glass. Applied Physics Letters 1999;74(6):812–4.
[10] Koster U, Meinhard J, Roos S, Rudiger A. Mater Sci Forum 1996;225-227:311.
[11] Murty BS, Ping DH, Hono K. Direct evidence for oxygen stabilization of icosahedral phase during crystallization of $Zr_{65}Cu_{27.5}Al_{7.5}$ metallic glass. Applied Physics Letters 2000;76(1):55–7.
[12] Inoue Akihisa, et al. Formation of icosahedral quasicrystalline phase in Zr-Al-Ni-Cu-M (M = Ag, Au or Pt) systems. Materials Transactions, JIM 1999;40(10):1181–4.
[13] Yong Zhang et al. Formation of Zr-based bulk metallic glasses from low purity of materials by yttrium addition. The Japan Institute of Metals 2000;1410–1.
[14] Liu CT, Wright JL, Walker LR, Kenik EA, Nieh TG, Paper presented at the UEF conference on Bulk Metallic Glasses, Singapore, 24–28 September 2000.
[15] Liu CT, White CL, Horton JA. Acta Metall 1985;33:213–29.
[16] Aoki, Izumi O. Trans Japan Inst Metals 1978;19:203.
[17] Liu et al CT. Test Environments and mechanical properties of Zr-base bulk amorphous alloys. Metallurgical and Materials Transactions A 1998;29A:1811–20.
[18] Mackay R, Miller GJ, Franzen HF. J Alloys Compounds 1994; 204:109–18.